4-2022

Observing and Exploring Intrinsic Characteristics of Type Ia Supernova

Connor Langevin

Observing and Exploring Intrinsic Characteristics of Type Ia Supernova

Connor Langevin

Undergraduate honors thesis under the direction of

Dr. Manos Chatzopoulos

Department of Physics and Astronomy

Submitted to the LSU Roger Hadfield Ogden Honors College in partial fulfillment of the Upper Division Honors Program.

April, 2022

Louisiana State University

& Agricultural and Mechanical College

Baton Rouge, Louisiana

Abstract

Using archival data from the Highland Road Park Observatory, in which the type Ia supernova ZTF20achlced was observed on six separate occasions from October to December 2020, apparent magnitude information was obtained. This was compared with apparent magnitude data from the Zwicky Transient Facility (ZTF). These apparent magnitude values were transformed into absolute magnitude, then luminosity values using the standard candle property of type Ia supernova and fit for their distance modulus using the SNooPy application in python. The luminosity values were then fitted to a luminosity vs time expression, which was then best-fit for unknown values of the supernova, such as the diffusion time scale and Nickel mass generated in the explosion. This paper found Nickel mass values in line with expectations for both data gathered from the Zwicky Transient Facility and from the Highland Road Park Observatory, and mostly within the expected range for the total ejecta mass and diffusion time scale.

Introduction

Type Ia supernova are predicted come from white dwarf stars whose mass rises above that of the Chandrasekar Limit (~1.4 solar masses). This increase in mass usually comes in the form of accretion from a companion star, which could lose its mass through a variety of processes. Once the Chandrasekar Limit is reached, the white dwarf will react violently and explode in a spectacular supernova; specifically, a type Ia supernova. Type Ia supernova luminosity curves tend to have (roughly) the same shape and peak luminosity as each other, which allows researchers to get accurate and precise distance measurements to these objects, even if they are millions of light years or even mega-parsecs away. This makes type Ia supernova fantastic

distance indicators (also known as standard candles due to their known brightness) to extremely far away objects in our universe, such as the supernova's host galaxy. Their known brightness also allows one to relatively accurately calculate the supernova's innate characteristics, such as how much radioactive Nickel was produced in the explosion or the diffusion time scale for the radiation to escape the expanding supernova ejecta.

The goal of this project was to observe type Ia supernova at Highland Road Park Observatory (HRPO), reduce all data obtained, and use this data to calculate certain characteristics of the observed supernova, such as the generated Nickel mass. Unfortunately, observed data at HRPO proved to be inconsistent and gave contradictory results, and so will be omitted. Therefore, archival data, which was also taken at HRPO, was used instead. This archival data was taken of the supernova "ZTF20achlced" from October to December 2020. This supernova is a known type Ia, and as such was perfect for analysis. Next, all raw data was reduced; this involved removing the dark and bias noise while factoring in the flats images for each night of data. This reduced data was then plate-solved and used for aperture photometry, where an apparent magnitude of the supernova was obtained for each night data was taken. This apparent magnitude was then transferred to absolute magnitude, which was itself then transitioned over to luminosity. Now, with luminosity and time data over the observation period, data could be fit to the luminosity model (**Figure 1/ Equation 1**), which was used alongside Scipy's curve_fit in python to best fit for the unknown parameters of the supernova, such as the

$$(1)\quad L(t) = \frac{2M_{\mathrm{Ni}}}{t_{\mathrm{d}}} e^{-\left[\frac{t^2}{t_{\mathrm{d}}^2}+\frac{2R_0 t}{v t_{\mathrm{d}}^2}\right]} \left[(\epsilon_{\mathrm{Ni}}-\epsilon_{\mathrm{Co}}) \int_0^t \left[\frac{R_0}{v t_{\mathrm{d}}}+\frac{t'}{t_{\mathrm{d}}}\right] e^{\left[\frac{t'^2}{t_{\mathrm{d}}^2}+\frac{2R_0 t'}{v t_{\mathrm{d}}^2}\right]} e^{-\frac{t'}{t_{\mathrm{Ni}}}} dt' \right.$$
$$\left. + \epsilon_{\mathrm{Co}} \int_0^t \left[\frac{R_0}{v t_{\mathrm{d}}}+\frac{t'}{t_{\mathrm{d}}}\right] e^{\left[\frac{t'^2}{t_{\mathrm{d}}^2}+\frac{2R_0 t'}{v t_{\mathrm{d}}^2}\right]} e^{-\frac{t'}{t_{\mathrm{Co}}}} dt' \right],$$

Figure 1: *Luminosity model used to fit the obtained data to a supernova light curve.*

created Nickel mass. Raw apparent magnitude data on the same supernova from the Zwicky Transient Facility (ZTF) survey was also used for comparison (Perley et al. 2020. p. 1-2).

Observations and Data Reduction

Archival observations taken from HRPO were used for all analysis and data reduction. This data was taken of the type Ia supernova ZTF20achlced from October to December 2020. This supernova reached a peak apparent magnitude of approximately 13.7 in late October. There were a total of six observations made, one of which was before the supernova's peak luminosity. The observations themselves were taken in three filters: R, V, and B. The B-Band filter was not used for any analysis past basic reduction, as the supernova was too faint to get reliable data in this filter. Of course, dark, bias, and flat frames were taken each night observations were made – for simplicity, the exposure time was kept constant at 60s for all images and noise frames.

The data reduction was a relatively straightforward process: The bias and dark frames were collected and averaged out to a combined bias and combined dark. The data reduction script was completed in the python coding language and the process to make a combined bias for a single night, for example, is shown below in **Figure 2**.

```
in_process_images = ccdp.ImageFileCollection(night_home)
bias_frames = in_process_images.files_filtered(imagetyp='Bias Frame', include_path=True)
combined_bias = ccdp.combine(bias_frames,
                             method='median',
                             sigma_clip=True, sigma_clip_low_thresh=5, sigma_clip_high_thresh=5,
                             sigma_clip_func=np.ma.median, sigma_clip_dev_func=mad_std,
                             unit = "adu"
                            )
combined_bias.write(os.path.join(R_path,'combined_bias.fit'), overwrite = True)
```

Figure 2: *Collecting all of the bias images from a single night and averaging all of them into a combined bias frame.*

The flat frames were taken in all three filters each night, and so needed to be separated and factored into the science images along with the combined bias and combined dark frames. This filtering and combination process is shown in **Figure 3**.

```
filters = ["B", "V", "R"]
combined_flats = {}
for y in filters:
    flat_frames = in_process_images.files_filtered(imagetyp='Flat Field', filter = "Bessel " + y, include_path=True)
    R_flats = []
    for flat_frame in flat_frames:    #They are different!
        image = CCDData.read(flat_frame ,unit = "adu")
        image = ccdp.subtract_bias(image, combined_bias)
        image = ccdp.subtract_dark(image, combined_dark, exposure_time = "exposure", scale = True,
                                   exposure_unit = u.s)
        #image = fpnfix.subtract_fpn(image, combfpn[60], mesh_size=32)
        R_flats.append(image)
    combined_flat = ccdp.combine(R_flats, scale = lambda x: 1/np.median(x),
                             method='median',
                             sigma_clip=True, sigma_clip_low_thresh=5, sigma_clip_high_thresh=5,
                             sigma_clip_func=np.ma.median, sigma_clip_dev_func=mad_std,
                             unit = "adu"
                            )
    combined_flat.write(os.path.join(R_path, f"combined_flats_{y}.fit"), overwrite = True)
    combined_flats["Bessel " + y] = combined_flat.copy()
```

Figure 3: *Code used to combine the bias, flat, and dark frames into a large combined "noise" frame. This was done for each filter, each night.*

This combined noise frame was then subtracted from the raw image, giving a reduced image. An example of which can be seen in **Figure 4**.

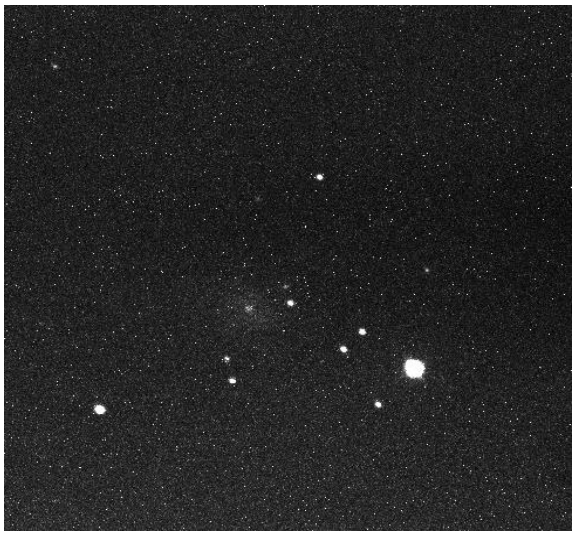

Figure 4*: Reduced image from October 14, 2020. The supernova is the bright object in image center.*

Plate Solving and Aperture Photometry

To get data out of these reduced images, they had to be plate solved. Plate solving is the act of mapping right ascension and declination coordinates (the sky coordinates) to locations on the image (pixel coordinates). This is also known as mapping to the World Coordinate System

(WCS). There are two primary methods of accomplishing this: automatically plate solving and manual plate solving. Automatic was definitely the preferred option if it was possible, and is basically the practice of using known bright stars around a given position in the sky to map to pixel coordinates. On poorer observation nights (cloudy, full moon, etc.) manual plate solving was required. This is the process of manually matching each star's known position in the sky with the pixel coordinates in the image. These stars usually came from that of the Gaia catalogue – an example of manual plate solving is shown in **Figure 5**. Once the plate solving was complete, the resulting image was in the form of a .wcs file – this allowed photometry on a target even if it was not picked up automatically, which was done by simply using the known RA and Dec sky coordinates of the supernova and transforming them into pixel coordinates.

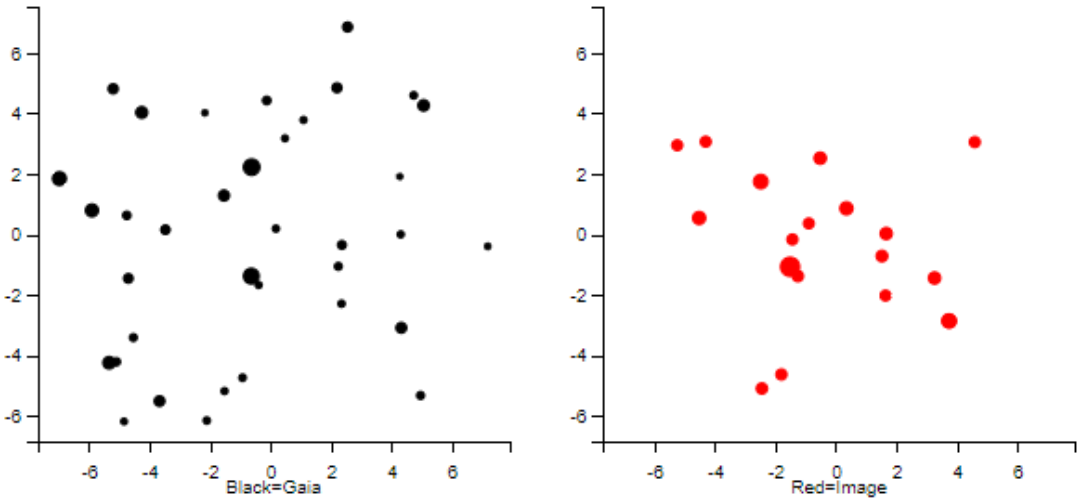

Figure 5: *All bright objects from* ***Figure 4*** *are on the right, whereas known bright stars around the same RA and Dec (given by the Gaia catalogue) are on the left.*

With the reduced image now plate solved, it was time to discern how bright each object in the image actually was. This was done by taking the pixel count values in an optimum aperture radius around each object. The optimum aperture radius is the radius around a given object in

which the signal to noise ratio is maximized. In other words, the pixel count of the stellar object is maximized whereas the background noise is minimized. **Figure 6** and **Figure 7** show optimum aperture radiuses for three arbitrary objects in a reduced image. These pixel count values, within the optimum aperture radius, are then added to achieve an instrumental magnitude for each object, each night. These instrumental magnitude values are virtually useless on their own for everything except brightness comparisons though! Therefore, to turn them into a useful quantity (apparent magnitude), a reference object with a known magnitude was needed.

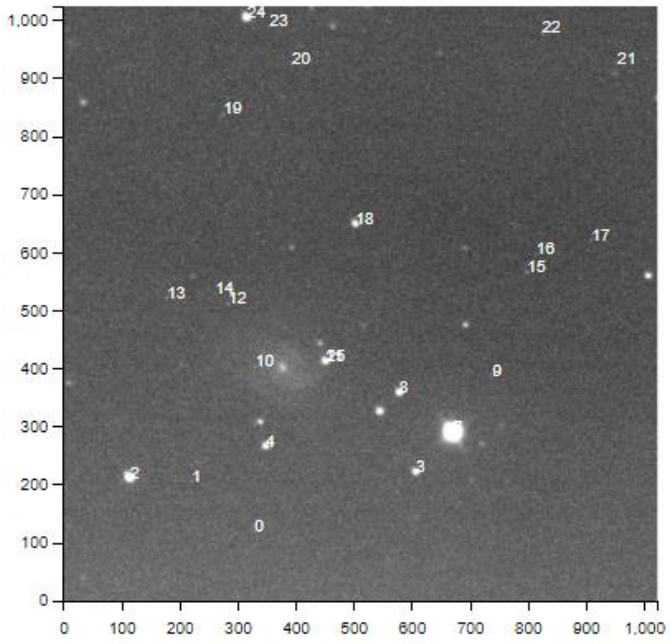

***Figure 6**: All objects bright enough to be automatically detected are listed here with an arbitrary identifier next to their position. Image from November 3, 2020.*

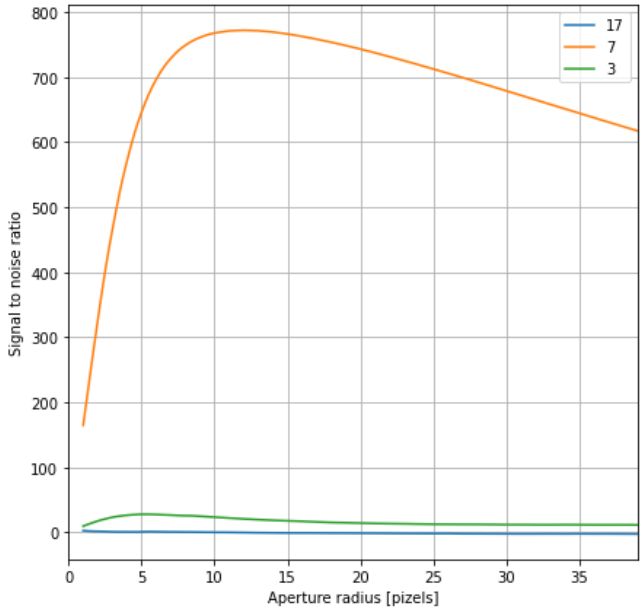

***Figure 7:** Objects 17, 7, and 3 are listed here with their signal to noise ratio as a function of their aperture radius. The optimum aperture radius occurs at the peak signal to noise ratio of each respective curve.*

A reference star was chosen based on its known magnitude (which was relatively close to that of the supernova) and its constant luminosity. This was object 3 in **Figure 6**, whose magnitude was given by the USNO URAT1 list as 14.55 in the R-Band and 14.81 in the V-Band. This star is also given by its Gaia DR2 identifier: 2586728377109575680 (Ochsenbein et al.

2001.). Subtracting the supernova's instrumental magnitude from that of the reference star, and then adding the known apparent magnitude of the reference star, yields the apparent magnitude, plots of which are shown below in **Figure 8** and **Figure 9** for the R and V filters, respectively. The raw ZTF data for apparent magnitude is also plotted in **Figure 10**, for comparison.

Apparent Magnitude to Luminosity

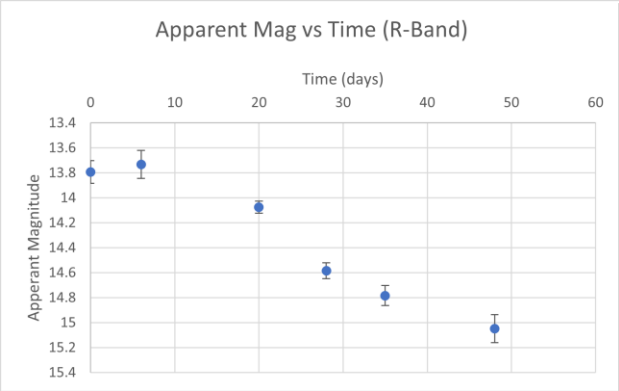

Figure 8: *Apparent magnitude, plotted as a function of time, over the HRPO observing period in the R-Band. Error bars are most likely underestimated. Day 0 is October 14, 2020.*

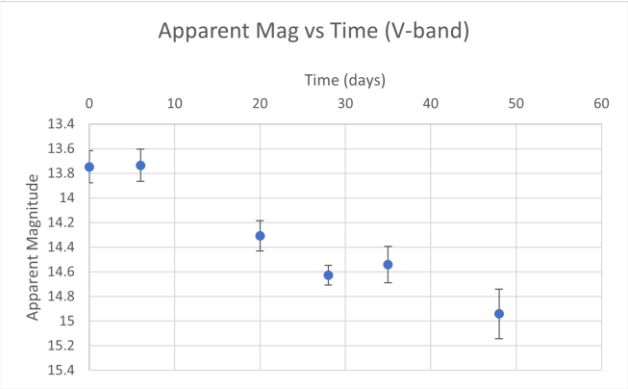

Figure 9: *Apparent magnitude, plotted as a function of time, over the HRPO observing period in the V-Band. Error bars are most likely underestimated.*

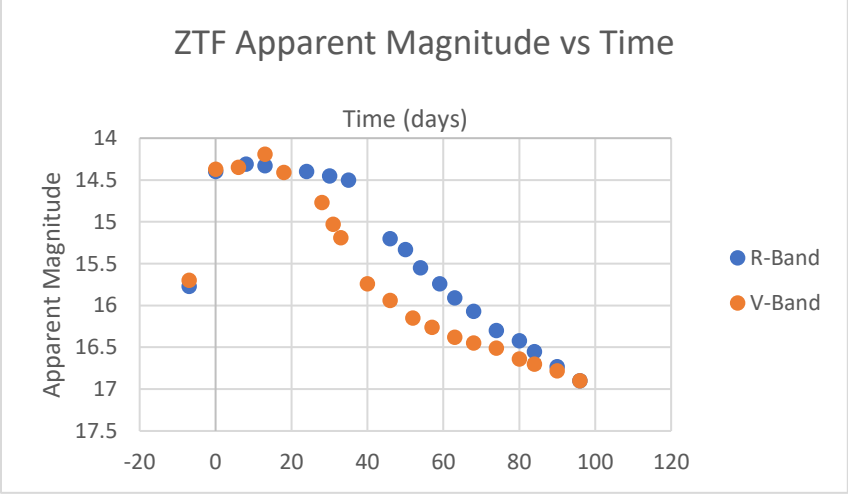

Figure 10*: ZTF apparent magnitude vs time in both the R and V bands. Error is extremely small on the ZTF data due to their precision and accuracy with multiple sources. Day 0 is October 14, 2020.*

With apparent magnitude, the next step was to convert to absolute magnitude, and from there luminosity. Apparent magnitude is related to absolute magnitude via the distance modulus expression:

$$m - M = \mu \quad (2)$$

Where m = Apparent Magnitude, M = Absolute Magnitude, and μ is the distance modulus. The distance modulus is a relation for the apparent and absolute magnitudes, including factors such as interstellar extinction and distance to the target. Since type Ia supernova's are standard candles, they all tend to peak at around the same value in absolute magnitude. Using this fact, we were able to fit for an approximation of the distance modulus, using the apparent magnitude from the R and V bands, using an incredible python resource called SNooPy (Burns, C. et al. 2011.). SNooPy allows one to fit for the distance modulus using apparent magnitude data from two different bands; in this case, R and V. SNooPy also factors in interstellar extinction using the given position of the supernova. SNooPy's resulting plot is shown in **Figure 11**.

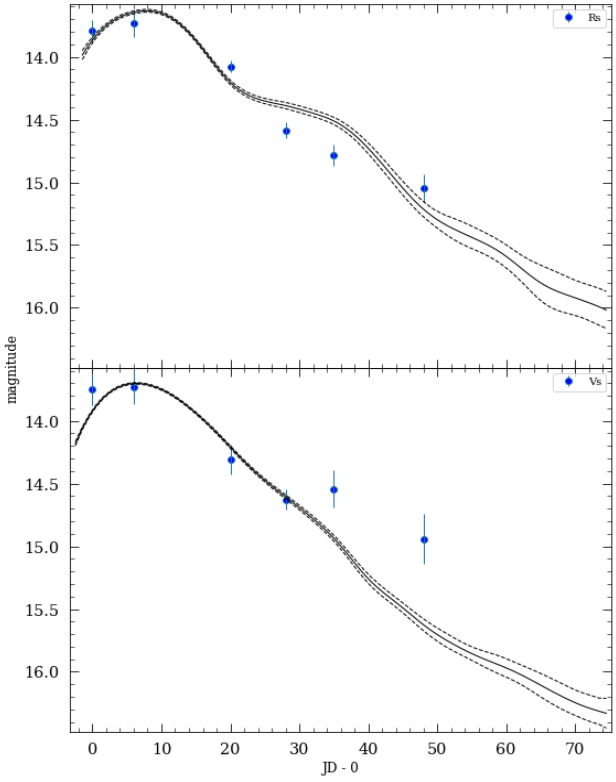

Figure 11: *SNooPy best fits for both the R (upper) and V (lower) band data from HRPO.*

The best fit distance modulus from SNooPy came out to 32.4 ± 0.3, which was then used to find the absolute magnitude. The uncertainty between the apparent magnitude and distance modulus values were propagated via putting the values in quadrature. The same procedure was repeated for the ZTF data; the resulting plots are shown in **Figures 12** and **13**.

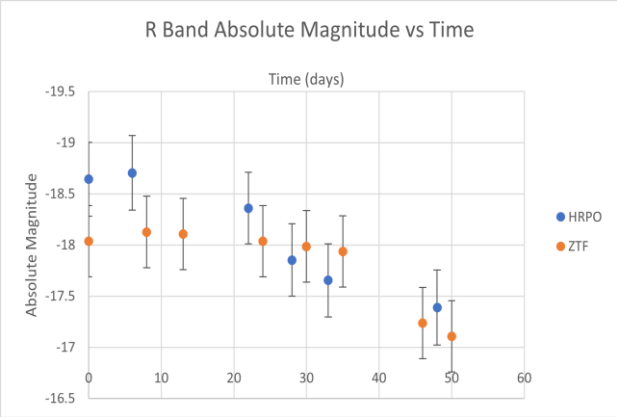

Figure 12: *R-band absolute magnitude values from HRPO and ZTF. Note that this is just the ZTF data over the 0 to 50 day time scale, the same period in which the HRPO data was taken.*

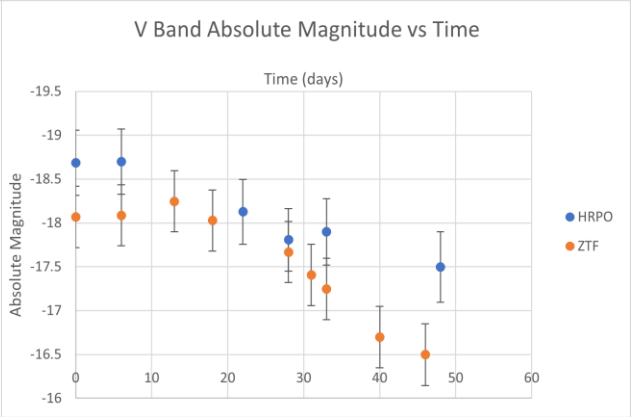

Figure 13: *V-band absolute magnitude values from HRPO and ZTF. Note that this is just the ZTF data over the 0 to 50 day time scale, the same period in which the HRPO data was taken.*

The absolute magnitude values were then converted to luminosity through **Equation 3**, below.

$$L^* = L^{\odot} 10^{0.4(M_{bol,\odot} - M_{bol,*})} \quad (3)$$

Where $L^{\odot}$ = 4E+33 ergs/s, $M(bol, \odot)$ = 4.74, and $M(bol, *)$ = the absolute magnitude plus a bolometric correction. For the purposes of the project, the bolometric correction was approximated to be 0 and as such, $M(bol, *)$ was approximately the absolute magnitude achieved from the ZTF and HRPO data. All absolute magnitude data was then put through this expression to obtain luminosity vs time, as can be seen in **Figures 14**, **15**, **16**, and **17**.

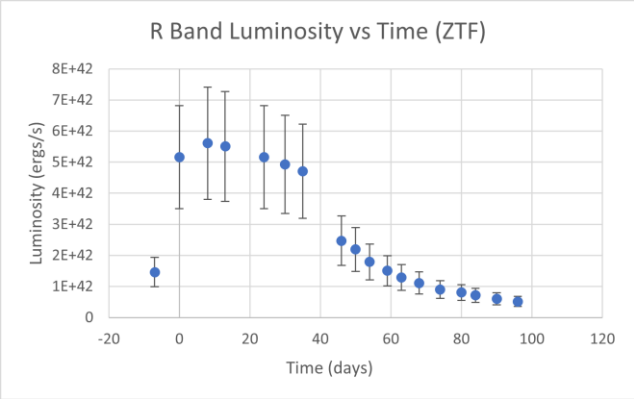

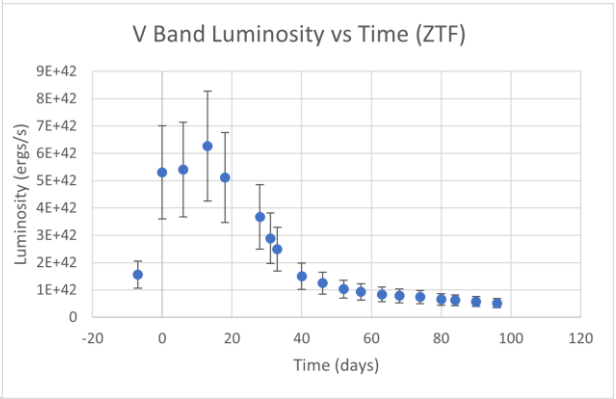

Figure 14: *R band luminosity vs time for all ZTF data over the ~100 day period.*

Figure 15: *V band luminosity vs time for all ZTF data over the ~100 day period.*

Fitting Luminosity for Unknown Parameters

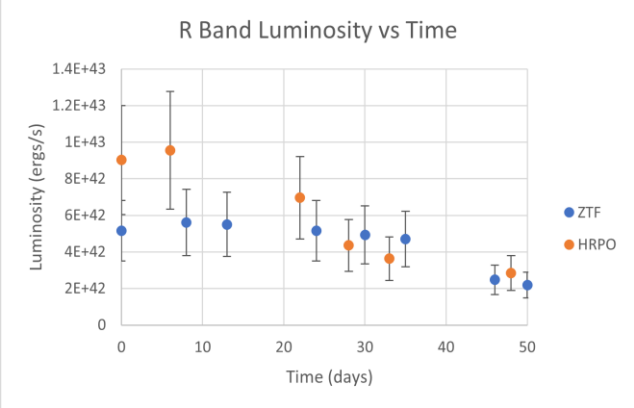

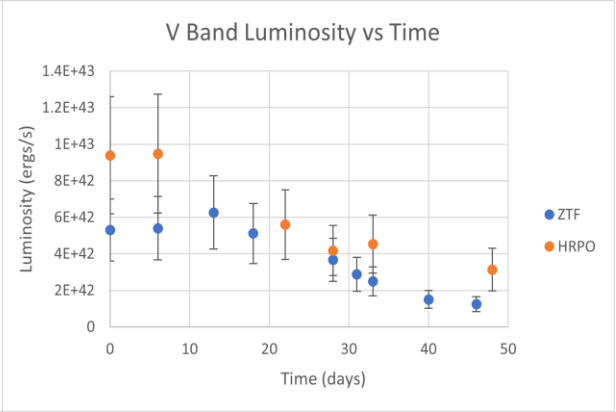

Figure 16: *R band luminosity vs time for all HRPO measurements and ZTF measurements taken between 0 and 50 days.*

Figure 17: *V band luminosity vs time for all HRPO measurements and ZTF measurements taken between 0 and 50 days.*

The above data was then thrust into the luminosity expression from **Figure 1**. A direct excerpt from the resulting code is also shown below in **Figure 18**. The luminosity expression was comprised of numerous constants, but firstly it should be stated that the approximation

```python
def rad_decay_dep(t,td,r0,vej):
    return ((r0*r15/(vej*td*day*kms2cms))+t/td)*np.exp((t/td)**2+(2.*r0*r15*t/(vej*kms2cms*(td**2)*day)))

def ni_dep_integ(t,td,r0,vej):
    return rad_decay_dep(t,td,r0,vej)*np.exp(-t/tni)

def co_dep_integ(t,td,r0,vej):
    return rad_decay_dep(t,td,r0,vej)*np.exp(-t/tco)

def Lum(x,Mni,td,r0,vej,A):
    res = (2.*Mni*Msun/td)*np.exp(-((x/td)**2+(2.*r0*r15*x/(vej*kms2cms*(td**2)*day))))* \
    ((eni-eco)*quad(ni_dep_integ,0,x,args=(td,r0,vej))[0] + eco*quad(co_dep_integ,0,x,args=(td,r0,vej))[0])* \
    (1.-np.exp(-A*A0/((x+0.01)*day)**2))
    return res

```

***Figure 18**: **Equation 1**, but shown in python, in chunks. Each integrand is separately calculated, then thrown together into the luminosity expression, "Lum".*

(Progenitor radius, or initial white dwarf star radius) $R_o \approx 0$ was used. This approximation could be made due to the fact that the expanding supernova ejecta so vastly eclipsed the initial size of the white dwarf star that for all intents and purposes the progenitor star radius was practically zero. Other constants include t_{Ni} = 113 days and t_{Co} = 8.8 days, which are the half-life timescales for radioactive Ni 56 and Co 56, respectively. $\epsilon_{Ni} = 3.9 \times 10^{10} \text{erg } s^{-1} g^{-1}$ and $\epsilon_{Co} = 6.8 \times 10^{9} \text{erg } s^{-1} g^{-1}$, which are the specific energies due to the radioactive decay of Nickel and Cobalt, respectively. $v = 10{,}000\ km/s$ and is the supernova ejecta velocity; it is usually taken to be between $5{,}000$ and $15{,}000\ km/s$, so the average was taken and used for analysis. This leaves the two values that were fit: t_d, the diffusion time scale for radiation to escape the expanding SN ejecta and M_{Ni}, the mass of radioactive Nickel produced in the explosion.

The integrands were integrated using scipy's quad.integrate function, which allows one to compute a definite integral over an interval (in this case, from 0 to t). The integration variable was denoted as x for purposes of simplicity but represents t' in **Figure 1**. The integrands were combined in one function, denoted "Lum", which then became the model to fit all luminosity and time data to.

Luminosity, luminosity uncertainty, and time values were pulled in via Numpy's "loadtxt" function, with two associated text files: "ZTF_Data" and "HRPO_Data". These values were loaded into the luminosity function ("Lum") using Scipy's curve_fit function, which uses a non-linear least squares fitting algorithm to fit the data. Curve_fit also recommends reasonable bounds and guesses for the fitted values: The bounds used were between 5 and 20 days for the diffusion time scale and between 0.05 and 1 solar masses for the Nickel mass. The guesses were 10 days for the diffusion time scale and 0.1 solar masses for the Nickel mass (Contardo, G. et al. 2000. p. 884). This can all be seen below in **Figure 19**, which is a direct snapshot of the curve_fit function implemented for the HRPO R-band data.

```
#R_HRPO
parameters, pcov = curve_fit(model, time_H, Lum_H_R, sigma = Uncert_H_R, p0=guess, bounds=bound)
M_Ni = parameters[0]
Diffusion_t = parameters[1]
```

Figure 19: *Scipy's curve_fit function being implemented over the model (**Equation 1**) Time_H (Time data for HRPO's R filter observations), Lum_H_R (Luminosity data over HRPO's R filter observations), p0 (guess values for the diffusion time scale and nickel mass), and bounds (bounds for the previously stated quantities).*

The last value to be obtained was the total ejecta mass. This was calculated from the diffusion time scale in **Equation 4** below, which is also directly represented in **Figure 20**.

$$M_{ej} = \frac{3}{10} * \frac{\beta c}{\kappa} v {t_d}^2 \tag{4}$$

A few more constants to get out of the way: β is simply an integration constant, equal to 13.7. c is the speed of light, approximately equal to $3 \times 10^8\ m/s$. κ is the optical opacity of the supernova ejecta, which tends to be between 0.1 and $0.3 \frac{g}{cm^2}$. Thus, the average was used: $0.2 \frac{g}{cm^2}$. Lastly, v is the aforementioned supernova ejecta velocity, taken to be $10{,}000\ km/s$, and

t_d is the diffusion time scale. As the total ejecta mass was calculated from the diffusion time scale, there was no need to set bounds or guesses for it.

```
Mej2 = ((3./10.)*(B*c/k)*V_ej*kms2cms*(parameters[1]*day)**2)/Msun
DMej2 = (Mej2*np.sqrt(4.*((pcov.diagonal()[1]/parameters[1])**2)))
print("HRPO R:")
print('M_Ni = ',parameters[0],' +/- ',pcov.diagonal()[0],' M_sun')
print('TD = ',parameters[1],' +/- ',pcov.diagonal()[1],' Days')
print('M_ej = ', ((3./10.)*(B*c/k)*V_ej*kms2cms*((Diffusion_t*day)**2))/Msun), ' +/- ', DMej2, "M_sun")
```

Figure 20: *Direct excerpt from how the total ejecta mass was calculated, along with its uncertainty, from the previous curve_fit expression in figure 19.*

Results of Fitted Quantities

All resulting values are shown in **Table 1**. This can be readily compared to **Table 2**, in which is listed example values for other, known type Ia supernova.

Unit:	(solar masses)	(solar masses)	(days)	(days)	(ergs/s)	(solar masses)	(solar masses)
	M_{Ni}	Error	t_d	Error	Log(Peak Lum)	M_{ej}	Error
HRPO, R:	0.330	0.007	7	9	43	0.1	0.3
HRPO, V:	0.334	0.007	7	8	43	0.1	0.3
ZTF, R:	0.154	0.001	20	11	42.7	1	1
ZTF, V:	0.123	0.002	19	11	42.8	0.8	0.9

Table 1: *Obtained values for the diffusion time scale and Nickel mass from the luminosity fit, as well as the calculated total ejecta mass and peak luminosity achieved. The peak luminosity values are present purely for a by eye comparison to the peak luminosity values in* ***Table 2****.*

It is immediately apparent that the Nickel mass error is likely underestimated and that the diffusion time scale's, on the other hand, is likely overestimated (And as byproduct, the total

ejecta mass' error as well). Even so, we can see a clear result that the HRPO R and V band data are consistent with one another in all expected values. However, it is also clear that the HRPO data is inconsistent with the ZTF data in terms of the expected Nickel mass, but consistent with the ZTF's range for the diffusion time scale. More surprisingly, the ZTF R and V band data are inconsistent with one another in terms of the expected Nickel mass, but consistent in terms of the diffusion time scale, as well as the total ejecta mass.

SN	$\log L_{bol}$ (erg s^{-1})	M_{Ni} ($M_\odot$)	$t_{-1/2}$ (days)
SN 1989B	43.06	0.57	12.9
SN 1991T	43.36	1.14	14.2
SN 1991bg	42.32	0.10	8.9
SN 1992A	42.88	0.37	10.6
SN 1992bc	43.22	0.84	13.2
SN 1992bo	42.91	0.41	9.9
SN 1994D	42.91	0.41	10.4
SN 1994ae	43.04	0.55	12.9
SN 1995D	43.19	0.77	12.9
SN 1998bu	43.18	0.77	13.1

***Table 2**: Peak luminosity, total Nickel mass, and diffusion time scale values for known type Ia Supernova (Contardo, G. et al. 2000. p. 884).*

These values can be readily compared to that in **Table 2**, which presents known diffusion time scales, peak luminosities, and Nickel masses for other type Ia supernova. Clearly apparent is the large range in which type Ia supernova Nickel masses and diffusion time scales lie; there is a clear range of 9 to 15 days for the diffusion time scale and 0.1 to 1.10 solar masses for the expected Nickel mass. The HRPO data lies within this expected range for the Nickel mass, but the uncertainty is too large on the diffusion time scale to say much more than the values are within the ballpark off the expected, if a little low. The ZTF data, as expected, lies within this range for the Nickel mass values, but the diffusion time scale is much higher than the expected range. Of course, with the relatively large error both the HRPO and ZTF diffusion time scales

present, it is difficult to draw conclusions other than that they are consistent with the expected values. Lastly, extrapolating the diffusion time scale values from **Table 2** into total ejecta mass values via **Equation 1** in **Figure 20**, gives us **Table 3**.

Here we can see a clear range in total supernova ejecta masses, with an average at 0.33 solar masses. The HRPO data has both the R and V bands with a total ejecta mass of 0.1 ± 0.3 solar masses. While the uncertainty is rather large, this is within the expected range for type Ia supernova, if a tad on the low side. The ZTF data, on the other hand, has the R band with a total ejecta mass of 1 ± 1 solar masses and the V band with 0.8 ± 0.9 solar masses. These values are certainly on the high end of the expected, but still within the range for a typical type Ia supernova.

	(days)	(solar masses)
SN	t_d	M_{ej}
1989B	12.9	0.38
1991T	14.2	0.47
1991bg	8.9	0.18
1992A	10.6	0.26
1992bc	13.2	0.4
1992bo	9.9	0.23
1994D	10.4	0.25
1994ae	12.9	0.38
1995D	12.9	0.38
1998bu	13.1	0.4

***Table 3**: Total ejecta mass values derived from **Table 2**, along with the diffusion time scale.*

Discussion and Conclusion

In summary, the HRPO and ZTF Nickel mass estimates derived from the luminosity model were both within the expected range for a typical type Ia supernova, even if error was underestimated in this portion. The diffusion time scales for the ZTF and HRPO unfortunately carried over plenty of error, but within this uncertainty we can see that both the ZTF and HRPO data was consistent with the expected, and with each other. This relation does not quite carry over to the

total ejecta mass, where we saw that the ZTF and HRPO data were found to be inconsistent with one another. Fortunately, they were both found in the expected range, if only on opposite ends.

There were several possible improvements that could be made to future iterations of this project, with the most important being the acquisition of more data. The HRPO observations were only taken six total days over an observation period of October to December 2020. This number could, and should, be improved dramatically to achieve much finer estimates for all derived and fitted quantities. From this, another important factor was observations before the peak of the supernova light curve; the HRPO had only taken one such data point, whereas the ZTF survey had only taken two. More brightness measurements before the peak would dramatically improve uncertainty estimates for all values. Also, brightness estimates in more filters than just R and V could be used; ideally the B band would be included as well. This would reduce uncertainty in the distance modulus calculation and thereby increase the accuracy of the final estimates.

Other improvements would include items such as the bolometric correction. It is difficult to say exactly how responsible the bolometric correction was for uncertainty, but it likely contributed a non-negligible amount. The obvious solution is to of course find the bolometric correction for your average type Ia supernova. Another, more subtle problem with this process has been the lack of comparison data. While there were the values shown in **Table 2**, that was practically the limit of publicly accessible, type Ia supernova Nickel mass and diffusion time scale estimates. More comparison data would give a much greater idea of the necessary comparison range for observed data, as well as a better idea for uncertainty estimates. Lastly, and the most obvious, would be to get more observations done on different type Ia supernova through this exact process. This approach would yield much better ideas for the correct values, and show

whether there might be a flaw in the model or with the observation equipment in regards to data from established catalogues, such as the ZTF.

Acknowledgments

I would like to thank the entire thesis committee and of course, Dr. Chatzopoulos especially, for their time and effort in helping my project be the best it could be. In addition, Dr. Penny greatly assisted in all forms of observations taken. Without him and the HRPO observatory, telescope observations and archival data use, let alone general data reduction, would have been impossible. I also must thank Jane Glanzer and Shania Nichols for their archival data and for allowing me to use it all! Lastly, Dr. Tabetha Boyajian for making necessary critiques of the thesis direction and for keeping me on course.

References

Perley, D. Fremling, C. et al. “The Zwicky Transient Facility Bright Transient Survey. II. A Public Statistical Sample for Exploring Supernova Demographics.” *Caltech University, University of Washington. et al*. 2020. June 2021. Website Link:

[2009.01242] The Zwicky Transient Facility Bright Transient Survey. II. A Public Statistical Sample for Exploring Supernova Demographics (arxiv.org)

Ochsenbein, F. et al. “The VizieR database of astronomical catalogues.” *Harvard University*. 2001. November 2021. Website Link:

VizieR (harvard.edu)

Burns, C. et al. “The Carnegie Supernova Project: Light-curve Fitting with SNooPy.” *Carnegie Institution for Science.* 2011. November 2021. Website Link:

The Carnegie Supernova Project: Light-curve Fitting with SNooPy - NASA/ADS (harvard.edu)

Contardo, G. et al. “Epochs of maximum light and bolometric light curves of type Ia supernovae.” *European Southern Observatory.* 2000. March 2022. Website Link:

2300876.DVI (springer.de)